RSC Advances

ROYAL SOCIETY OF CHEMISTRY

www.rsc.org/advances

A novel electrochemical hydrogen peroxide biosensor based on hemoglobin capped gold nanoclusters-chitosan composite

MojtabaShamsipur[a]*, AfshinPashabadi[a], Fatemeh Molaabasi[b]

A biocompatible nanocomposite containing hemoglobin capped gold nanocluster (Hb-AuNCs) and chitosan was prepared and applied to the modification of a glassy carbon electrode (GCE) for preparation of a highly sensitive hydrogen peroxide biosensor. The electrochemical behavior of Hb-AuNCs in the composite film was studied in phosphate buffer solution of pH 7.4 and a pair of quasi-reversible redox peak attributed to the electrode reaction of Hb's Fe(III)/Fe(II) redox couple was observed. The FTIR and UV-Vis spectroscopy indicated that Hb entrapped in the composite film possesses substantial changes in its secondary structure so that it provided a high peroxidase-like enzyme activity attributing to the excellent electrical conductivity of the encapsulated gold nanoclusters. The AuNCs found to play a critical role as conductive holder and accumulator of redox active centers at the surface of GCEs. The fabricated biosensor showed fast response, acceptable stability, excellent sensitivity, and high electrocatalytic activity toward the reduction of hydrogen peroxide. The oxidation peak current was found to be linearly proportional to H_2O_2 concentration in the range of 55- 700 nM with a limit of detection of 16.5 nM (at S/N=3).

Keywords: Hemoglobin, Gold nanoclusters, Electrocatalysis; H_2O_2 detection

---

[a] *Department of Chemistry, Razi University, Kermanshah, Iran, E-mail: mshamsipur@yahoo.com; Fax: +98 21 66908030; Tel: +98 21 66906032*

[b] *Department of Chemistry, Tarbiat Modares University, Tehran, Iran*

Introduction

Recently, there is an increasing interest in development of an electrochemical basis for investigations of protein structure, mechanisms of redox transformation of protein molecules and their metabolic processes involving redox transformations. Understanding of these reactions fundamentally can provide an insight into physiological electron transfer process as well as an impetus to the further development of biosensors and bio-electrocatalytic systems.[1-3] In this line, there has been much effort for development of H_2O_2 electrochemical biosensors which can widely improve the understanding of the redox processes of enzymes and proteins, and their transport and bioavailability.[4] H_2O_2 is not only known for its cytotoxic effects and associated tissue injury, but also plays a key role in physiological and biomedical studies and in monitoring of biological processes. H_2O_2 is also a side product of many oxidative biological reactions catalyzed by enzymes such as glucose oxidase (GOx), lactate oxidase (LOx), cholesterol oxidase (ChoOx), etc.[5] Therefore, sensitive and accurate determination of H_2O_2 is of vital importance in many biological applications.

Hemoglobin (Hb), a typical multi-cofactor protein that possesses two heme-containing dimers, is considered to be an ideal model protein for the study of electron transfer of heme containing molecules, because of its commercial availability, moderate cost and well-known structure.[6] Moreover, due to its intrinsic peroxidase activity, Hb can be used in the design of H_2O_2 biosensors.[5,7] However, it has been documented that, on conventional solid electrodes, the fast electron transfer between Hb and the electrode is not possible because the redox center of proteins is embedded in polypeptide chain structures and the proteins are easily absorbed on the electrode surface.[8] Such slow electron exchange may be due to unfavorable orientation of Hb molecules on electrode surfaces, which increases the distance between its heme center and electrode surface, and also to the adsorption of impurities and denatured proteins onto electrode surface, which can block the electron communication between heme and electrode.[9] Therefore, great efforts have been devoted to explore new immobilization methods and supporting materials that accelerate the electron transfer of Hb while maintaining its enzymatic activity. In this respect, the selection of appropriate nanomaterials (NMs), including nanoparticles (NPs),[10,11] quantumdots (QDs)[12,13] and carbon nanomaterials[14,15] is an important issue for fabrication of an effective electrochemical biosensor based on Hb as a cheap mimetic enzyme.

Recently, the protein-supported nanoclusters of noble metals with excellent conductivity have been successfully applied as electrochemical interfaces for sensitive detection of H_2O_2,[16] glucose,[17] retinal-binding protein[18] and KB cells.[19] In recent years, we have been involved in one-pot 'green' synthesis of fluorescent Hb-AuNCs with reactive functional groups, low-toxicity, good biocompatibility and stability.[20] We also found that Hb remains active in the Hb-AuNCs as an excellent sensing platform for hydrogen peroxide, which makes the nanocuster attractive for further investigation in different analytical fields including electrochemical applications.[21]

On the basis of the above findings, herein, we employed Hb-AuNCs as a non-enzymatic electrochemical probe for a very simple and convenient preparation of a biosensor for H_2O_2 with enhanced electrocatalytic activity. In one hand, the AuNCs can induce substantial conformational changes of Hb while keeping its bioactivity on electrode and, in the other, the encapsulated AuNCs possess very important role in enhancing the rate of electron transfer in Hb, which results in improved electrochemical sensing ability. To the best of our knowledge, this is the first time that the direct electrochemistry of Hb-AuNCs and its electrocatalysis towards H_2O_2 has been investigated in a sensing system.

Experimental

Chemicals

Human hemoglobin (Hb, MW 66,000) was purchased from Sigma and used without further purification. Hydrogen tetracholoroaurate ($HAuCl_4$) was obtained from Alfa Aesar and trisodium citrate, sodium hydroxide and ammonia were purchased from Fluka. The experimental procedures for preparation of hemoglobin were carried out based on the protocol of Williams and Tsay[22] and its concentration was monitored by the method of Antonini and Brunori (ε_{415nm} = 125 mM^{-1} cm^{-1} or ε_{541nm} = 13.8 mM^{-1} cm^{-1} per heme),[23] as reported before.[20,21] 5 mg mL^{-1} hemoglobin solutions of pH 7.4 were stored at 4 °C. 0.1 M phosphate buffers of various pH values were prepared by mixing the stock solutions of Na_2HPO_4 and NaH_2PO_4 and adjusted by 0.1 mM NaOH and 0.1 mM H_3PO_4 solutions. All other chemicals were of analytical grade from

Merck and used without further purification. All solutions were made up with doubly distilled water.

Apparatus

The electrochemical experiments were performed using an Autolab modular electrochemical system (ECO Chemie, Ultrecht, The Netherlands) equipped with a PGSTAT 101 module and driven by NOVA software (ECO Chemie) in conjunction with a personal computer for data storage and processing. The electrochemical cell used was consisted of a three-electrode system using the modified glassy carbon electrode (GCE, d=3.0 mm) as the working electrode, a platinum wire as a counter electrode and an Ag/AgCl electrode as the reference electrode. Air was injected into deoxygenated phosphate buffer solution by syringe under nitrogen atmosphere. Amperometric experiments were carried out in a stirred system by applying an analytical potential to the working electrode. Aliquots of H_2O_2standard solution were added successively to the solution. Current-time data were recorded after a steady state current had been achieved. Faradaic impedance measurements were performed in the presence of a 1:1 mixture of 5 m$MK_3Fe(CN)_6/K_4Fe(CN)_6$ as a suitable redox-probe, using an alternating current voltage of 10 mV and frequency range of 0.01 to 10000 Hz. The UV–vis and IR spectra were recorded on an UV-2450 UV–vis recording spectrophotometer (Shimadzu, Japan) and a Tensor 27 Bruker instrument (Bruker, Japan), respectively. The TEM images were recorded using a Philips CM30 transmission electron microscope with accelerating voltages of 80 and 150 kV. Samples were prepared by drop casting solution on carbon coated copper grids and dried at room temperature. All pH measurements were performed at 25.0 ± 0.1 ºC by using a Metrohm 713 pH/ion-meter with a standard uncertainty of 0.1 mV (Metrohm, Switzerland).

Synthesis of hemoglobin-capped AuNCs

All glassware was thoroughly cleaned with aqua regia (HNO_3/HCl, 1:3) and rinsed extensively with ethanol and Milli-Q water (resistivity >18 MΩ cm) prior to use. The generation of blue emitting Hb-AuNCs was mainly based on previously established synthetic methods.[20,21] In brief, a 5 mL aqueous solution of $HAuCl_4$ (2.8 mM, 37 °C) was reacted with 5 mL of human adult

hemoglobin (Hb) (7 mg mL^{-1}, 37 °C), under vigorous stirring. After 10 min, 1.0 mL of NaOH solution (1 M) was introduced and the reaction was allowed to proceed under vigorous stirring at 37 °C for 24 h. After centrifugation (12,000 rpm, 10 min, 4 °C) to remove any suspended particles and byproducts with larger particle sizes, the blackish green solution of the as-prepared Hb-AuNC was collected and kept at 4 °C before use. The concentration of Au nanoclusters was calculated by the concentration of the Hb in Hb-AuNCs solution.[24] The concentration 5.5×10^{-5} M of Hb-Au nanoclusters was measured spectrophotometrically using a molar absorptivity of 131936 M^{-1} cm^{-1} at 280 nm. The particle size and shape of Hb-AuNPs were evalualuated by transmission electron microscope (TEM). The TEM image of AuNCs@Hb is shown in Fig. 1. It can be seen that the AuNCs are well-dispersed with spherical shapes with an average size of 2.5±0.6 nm.

(Fig. 1)

Preparation of biosensor

A GCE (d=3 mm) was polished to a mirror-like surface with 0.3 and 0.05 μm aluminum slurry, respectively. Subsequently, the electrode was rinsed with 1:1 HNO_3–H_2O (v/v), ethanol and doubly distilled water in an ultrasonic bath for 2–3 min for each wash and dried under nitrogen at room temperature. Chitosan (Chit) was dissolved in 1.0% (v/v) acetic acid solution and stirred for 2 h to form 0.5% (w/v) solution at room temperature. After filtering out of the un-dissolved materials, the pH was adjusted using 1.0 M NaOH. Then the Hb-AuNPs/Chit composite biosensor was prepared with the following procedure: 8 μL of the colloidal Hb-AuNPs solution was cast at on the surface of GCE, and the electrode was dried in air. Finally, 12 μL of the as-prepared chitosan solution was cast on the surface of fabricated modified electrode and dried in air.

Results and discussion

FTIR study

Since proteins have conformation sensitive spectral signature in the infrared region of the electromagnetic radiation, the FTIR was employed as a suitable technique to identify the conformational sensitive binding sites with the nanoparticle. Fig. 2A shows a comparison between the FTIR spectra of Hb (a) and Hb-AuNCs (b). Compared with the pure IR spectra of Hb (a), the intensity of amide I (1650 cm^{-1}) of Hb immobilized on Hb-AuNCs (b) is decreased, and amide II (1533 cm^{-1}) is disappeared, in the expense of the appearance of a rather sharp band at 1436 cm^{-1} (Fig 2A). The results indicated that the gold nanoclusters present in the prepredHb-GNCs induce a conformational change of the secondary structure of the protein.[20] Moreover, the 1436 cm^{-1} band is due to the vibration of tryptophan (Trp) that becomes drastically larger when nanoclusters are prepared at high pH.[25]

UV–vis spectroscopy

It was important to know whether heme-protein maintained its natural state in composite film. It is well known that position of the Soret absorption band of prosthetic heme group provided information about possible denaturation of heme-proteins.[25] The UV–visabsorption spectroscopy was then employed for the conformation study of Hb in composite film (Fig. 2B). It is quite obvious from Fig. 2B that the Soret band of Hb alone (curve a) is located at about 412 nm, but in the presence of AuNCs (curve b), it is shifted to 403 nm while its intensityis significantly decreased. These results indicate that the formation AuNCs in the presence of Hb leads to the unfolding of the protein skeleton.[20] In addition, the increase in intensity of a bandaround 215 nm (related to the α-helix structure of the protein) and the disappearance of bands located at 280 nm (due to the phenyl group of Trp and tyrosine residues), and 540 and 575 nm (related to oxy-band or Q-band) confirm that the microenvironment surrounding heme in Hb-AuNCs is different from that of native Hb.[20,26]

(Fig. 2)

EIS study

EIS is a commonly used method to probe the interface information of the impedance changes during the stepwise-assemble process of the surface modified electrode.[27-29] In EIS the semicircular part at higher frequencies corresponds to the electron transfer limited process and the linear part at lower frequencies corresponds to the diffusion process. The value of charge transfer resistance (R_{ct}) can be estimated according to the diameter of the semicircle of the Nyquist plots at the high frequency region, which controls the electron transfer kinetics of redox probe at the electrode surface and reflects the interfacial electron transfer ability.

Fig. 3A shows the impedance spectra represented as Nyquist plots (Z″ vs. Z‘) for bare GCE (a) and Hb-AuNCs/Chit/GCE (b) in 5 mM$Fe(CN)_6^{3-/4-}$ containing 0.1 M KCl solution with the frequency sweep from 105 to 0.1 Hz. Here Z' and Z″ are the real and the imaginary variables of impedance. The representative Randles circuit for the Nyquist plots is shown in inset of Fig. 3A, where R_s, CPE, R_{ct} and W represent solution resistance, a constant phase element corresponding to the double layer capacitance at the electrode surface, the charge transfer resistance and the Warburg impedance, respectively. The diameter of the semi-circle is proportional to the charge transfer resistance; hence, the electron transfer properties can be determined accordingly. The straight line portion represents the Warburg impedance which takes into account the frequency dependence on diffusion transportation to the electrode surface. As is shown, there is a very low charge transfer resistance for $Fe(CN)_6^{3-/4-}$ at bare GCE (curve a). However, after modifying the GCE with Hb-AuNCs/Chit film, the R_{ct} increases dramatically to about 2000 Ω (curve b), as obtained from the corresponding Randles circuit, indicating that the biocomposite film hinders the charge transfer process.

It should be noted that the plot of Z‘ at Warburg portion vs $\omega^{-1/2}$ (Fig. 3B) can also be applied to determine R_{ct}. The obtained value of R_{ct} from the intercept of the linear Z‘ vs $\omega^{-1/2}$ plot[27] was found to be 1998 Ω, which nicely confirms the obtained value of 2000 Ω from the corresponding Nyquist plot.

(Fig. 3)

Direct electrochemistry of Hb-AuNCs and electrocatalysis of H_2O_2

In order to compare the electrochemical properties of Hb and Hb-AuNCsfilm, the cyclic voltammograms of Hb/Chit/GCE and Hb-AuNCs/Chit/GCE in 0.1 M PBS of pH 7.4 at a scan rate of 50 mV s^{-1} were recorded. As shown in Fig. 4 curve a, when the electrode was modified with Hb/CHIT film, only a unsymmetrical quasi reversible weak peak for Fe(III)-porphyrin ↔ Fe(II)-porphyrin redox reaction with a ΔE_p of about 174 mV was observed, indicating that the direct electron transfer rate of Hb with GCE is very slow and only few Hb molecules closest to the electrode surface could exchange electrons. However, at the Hb-AuNCs/Chit/GCE an enhanced redox peak with much lower ΔE_p of 130 mV was observed (curve b). The formal potential (E°′), estimated as $(E_{pa}+ E_{pc})/2$, where E_{pa} and E_{pc} are the anodic and cathodic peak potentials, respectively, is -0.285 vs. Ag/AgCl. It is interesting to note that this value is more positive than the corresponding literature reported values for Hb/C60–NCNTs/CHIT/GCE (−0.335 V vs. SCE),[30] Hb/RTIL/PDDA-G (−0.326 V vs. SCE),[31] Nafion/Hb/PAM-P123/GCE (−0.317 V vs. SCE),[32] Hb/AgNPPdop@CNP/GCE (−0.398 V vs. SCE),[33] Hb/HNTs/ILs-modified electrodes (−0.313 V vs. Ag/AgCl);[34] while, it is more negative than that reported for GCE/CM-DDAM@Hb (−0.186V vs. Ag/AgCl)[35] and Hb/Chit-[bmim]PF6-Gr/GCE (−0.206V vs. SCE).[36]

As is obvious from Fig. 4, here the charging current increased, due to the increased active surface and 3D structure of Hb-AuNCs which confers a much higher electrochemical activity to the modified electrode. As can be seen, at Hb-AuNCs/Chit film, the electrochemical response of Hb is greatly enhanced, indicating that the AuNCs play a key role as conductive holders and accumulators of the redox active centers (RACs) at the surface of glassy carbon electrode. Thus, as expected, the capability of AuNCs in improving the electron transfer rate of Fe(II)/Fe(III) redox reaction resulted in enhanced sensitivity of the biosensor due to increased density of the RACs, relative to the simple Hb/Chit modified electrode.

(Fig. 4)

In order to compare the electrocatalytic activity of Hb/Chit/GCE and Hb-AuNCs/Chit/GCE, their responses to the reduction of H_2O_2 was explored. Typical cyclic voltammograms of Hb/Chit/GCE and Hb-AuNCs/Chit/GCE in 0.1 M PBS solution of pH 7.4 in the presence of 12.0 µM of hydrogen peroxide at a scan rate of 50 mV s^{-1} are presented in Fig. 4,

curves a′ and b′, respectively. As is obvious from curve a', the addition of H_2O_2 to the electrochemical cell resulted in an increase in the reduction peak at -0.35 V accompanied by a distinct decrease in the oxidation peak, emphasizing a typical electrocatalytic reduction process for H_2O_2. Moreover, as expected, the electrocatalytic current at Hb/Chit/GCE for H_2O_2 (curve b') found to be much lower than that at Hb-AuNCs/Chit/GCE (curve a'), which is attributed to the small RACs density at Hb/Chit/GCE.

As is obvious from Fig. 4, in the presence of hydrogen peroxide, the Fe(III)↔Fe(II) onset potential was slightly delayed. This is most probably due to the higher electron transfer resistance of active centers which causes the absorption hydrogen peroxide on the Fe(III) active center to some extent. The results thus obtained demonstrated that the presence of AuNCs at the electrode surface results in the increased efficiency of immobilization. The high efficiency of AuNCs in charge transfer can uphold number of Hb molecules that can be reduced/oxidized, simultaneously. According to the literature,[37] the heme can react with H_2O_2 to first form an intermediate (compound 1 in Fig. 5), which in turn, possesses a high catalytic activity towards H_2O_2. Accordingly, a plausible catalytic pathway is explained in Fig. 5.

(Fig. 5)

Effect of scan rate

Fig. 6A shows the cyclic voltammograms of Hb-AuNCs/Chit/GCE modified electrode in 0.05 M PBS of pH 7.4 at different scan rates from 20 to 500 mV s^{-1}. It can be seen that the redox peak currents increase linearly with scan rates over the range studied (Fig. 6B), indicating that the pair of redox waves originates from the surface confined molecules. The respective linear regression equations between the oxidation and reduction peak currents and scan rate were calculated as: I_{pa} (μA) = 3.739 υ (V s^{-1}) + 0.188 (R^2 = 0.993) and I_{pc}(μA) = -4.697 υ (V s^{-1}) - 1.002 (R^2 = 0.994), respectively. This observation suggested that the redox process of Hb over the prepared sensor was surface-controlled. Meanwhile, the redox peak potential was shifted slightly with increasing scan rate so that the peak-to-peak separation was increased gradually, clearly indicating a quasi-reversible electrochemical process.

The redox peak potentials exhibited linear relationship with natural logarithm of scan rate (ln υ) in the range from 20 to 500 mV s^{-1} with the regression equations E_{pa} (V) = 0.068 ln υ - 0.083 and E_{pc} (V) = -0.049 ln υ - 0.511, respectively. By using the above regression equations for E_{pa} and E_{pc}, the electrochemical parameters of Hb in the hybrid film were evaluated according to the following Laviron's equations:[38,39]

$$E_{pc} = E^{0'} - \frac{RT}{\alpha nF}\ln \upsilon \quad (1)$$

$$E_{pa} = E^{0'} - \frac{RT}{(1-\alpha)nF}\ln \upsilon \quad (2)$$

$$\log k_s = \alpha \log(1-\alpha) + (1-\alpha)\log \alpha - log\frac{RT}{nF\upsilon} - \frac{(1-\alpha)\alpha nF\Delta Ep}{\alpha nF} \quad (3)$$

where, α is the electron transfer coefficient, n is the number of electron transferred, υ is the scan rate, and $E^{0'}$ is the formal potential, k_s is the electron transfer rate constant and ΔE_p is the peak-to-peak potential separation and R, T and F have their conventional meanings. The values of α and k_s were then calculated as 0.52 and 0.85 s^{-1}, indicating a fast electron transfer rate with high efficiency.

(Fig. 6)

By further use of the effect of the scan rate on the electrochemical response of Hb-AuNCs/Chit/GCE (Fig. 6B) and use of the following standard equation:[38]

$$I_{pc} = \frac{n^2F^2\upsilon A\Gamma}{4RT} = \frac{n\,F\,Q\upsilon}{4RT} \quad (4)$$

where Q is the charge involved in the reaction which is equal to nFAΓ, n is the number of electron transferred (n=4 for Hb), F is the Faraday constant, and A is the electrode area (cm^2), the surface coverage (Γ) of the electroactive Hb in the modified electrode was estimated for the GCEs modified with Hb-AuNCs/Chit and of Hb/Chit as 3.8×10^{-9} and 3.2×10^{-10} mol cm^{-2}, respectively. These values were found to be larger than that of the theoretical monolayer coverage of 1.89×10^{-11} mol cm^{-2},[40] suggesting that more than one layer of Hb is participating in the electron transfer process and also show that the RACs of Hb-AuNCs nanomaterial immobilized electrode is more than that of simple Hb one, under the same dispersed concentration of Hb.[15]

Effect of pH

The solution pH is essential to the electrochemical behaviors of proteins. Because its proton participated in the redox process, the immobilized Hb shows a strong dependence on solution pH (Fig. 7). Asis obvious from Fig. 7, in the pH range of 3.5–10.0, the peak potentials shifted negatively and the maximum peak currents obtained at pH 7.4. Therefore, a PBS solution of pH 7.4 was use in further studies. The electrochemical reaction can be expressed as: HbFe(III) + H^+ + e^- ⇌ HbHFe(II). Thus, the reason for the above mentioned pH effect might be the influence of the protonation states of trans ligands to the heme iron and amino acids around the heme, or the protonation of the water molecule coordinated to the central iron.[41]

(Fig. 7)

Amperometric study

To evaluate the practical applicability of the designed Hb-AuNCs/Chit/GCE system, H_2O_2 was selected as an important reagent to examine the biocatalytic ability of the Hb-AuNCs. Fig. 8A shows the steady-state current response of H_2O_2, at a constant electrode potential of -0.3 V. As seen, during the successive addition of hydrogen peroxide, a well-defined response is observed. The plot of response current vs H_2O_2 concentration (Fig. 8B) was linear over the concentration range 55 to 700 n M, with a linear regression equation of I (μA) = -0.351 [H_2O_2] (nM) – 20.064 (R^2 = 0.9961) and a limit of detection (LOD) of 16.5 nM (at S/N=3). As is obvious, the developed method shows high sensitivity and wide linear range, and possessing the potential to be one of the most commonly used analytical methods for detection of very low concentration of H_2O_2.

(Fig. 8)

The apparent Michaelis-Menten constant (K_M^{app}), which provided to be an indication of the enzyme substrate kinetics, was calculated from the electrochemical version of the Lineweaver-Burk equation:[42]

$$\frac{1}{I_{SS}} = \frac{1}{I_{max}} + \frac{K_M^{app}}{I_{max}C} \quad (5)$$

Where I_{ss} is the steady current after the addition of substrate, C is the bulk concentration of the substrate, and I_{max} is the maximum current measured under the saturated substrate condition. K_M^{app}, obtained by the analysis of the slope and the intercept of the plot of the reciprocals of the steady-state current vs H_2O_2 concentration, was found to be 124 μM, which is much smaller than those of 369 μM for the Hb/HNTs/ILs/GCE,[43] 896 μM for Hb/Chit film-modified carbon paste electrode[44] and 490 μM for the Hb/cationic clay-modified GCE electrode.[45] The small value of K_M^{app} indicates that the immobilized Hb entrapped on the proposed biosensor exhibits higher enzymatic activity and a high affinity for H_2O_2.

Stability, repeatability and effect of potential cycling

The modified electrode showed an acceptable stability and repeatability. When not in use, the modified electrode was stored in pH 7.4 PBS at 4 °C for about 3 weeks, and found to retain about 94% of its initial current response. The relative standard deviation (RSD) was 6.4% for nine successive determinations of a 500 nM H_2O_2 with the modified electrode. The fabrication of seven modified electrodes, made independently, showed a good reproducibility with RSD of 7.2% for the current determined in the presence of 50 nM H_2O_2. Continuous potential cycling between -0.8 and 0.1 V in 0.05 M PBS of pH 6.8 was used for the investigation on the stability of modified electrode. As it is seen from Fig. 9, after 80 continuous cycles at a scan rate of 50 mV s^{-1}, the peak heights of the cyclic voltammograms did not show any considerable change.

(Fig. 9)

Comparison of linear range and limit of detection of different H_2O_2 sensors

Table 1 compares the linear range and LOD of the proposed Hb-AuNCs/Chit/GCE with those of some of the best enzymatic[46-48] and nonenzymatic[49-60] elerctrochemical hydrogen

peroxide sensors, very recently reported in the literature. As is obvious from the summarized data, the proposed amperometric biosensor can be ranked among a few of the best reported H_2O_2 sensors, from the viewpoints of linear range and LOD.[46,47,54,61] Moreover, the fabricated biosensor showed very fast response, acceptable stability, excellent sensitivity, and high electrocatalytic activity toward the reduction of hydrogen peroxide. To the best of our knowledge, this is the first time that the direct electrochemistry of Hb-AuNCs and its excellent electrocatalytic property towards reduction of H_2O_2 has been investigated in a sensing system. Meanwhile the results obtained from this work emphasized that the Hb-AuNPs/Chit film possesses a promising potential in fabricating the third generation of nonenzymatic electrochemical biosensors, bioelectronics, biocatalysis and biomedical devices in the future.

Conclusions

In this work, direct electrochemistry of Hb-AuNCs was investigated when the protein capped gold nanoclusters were immobilized by Chit on a GCE. The AuNCs play a role as conductive holder and accumulator of redox active centers (RACs) at the surface of glassy carbon electrode. The high RACs density of the prepared Hb-AuNCs/Chit/GCE biosensor increased its sensitivity considerably as it was compared with a simple Hb/Chit/GCE. Excellent electrocatalytic properties of the modified electrode toward hydrogen peroxide indicated that the films possess a promising potential in fabricating the third generation nonenzymatic electrochemical biosensors, biocatalysis, bioelectronics and biomedical devices in the future.

Acknowledgements

The authors thank Iran National Elite Foundation (INEF), Research Council of Razi University and Center of Excellence in Sensors and Biosensors at Razi University for the support of this work.

References

1 Q. I. Wang, G. X. Lu and B. J. Yang, Myoglobin/sol–gel film modified electrode: directelectrochemistry and electrochemical catalysis, *Langmuir*, 2004, **20**, 1342–1347.

2 J. X. Li, L. H. Zhou, H. Xia, J. Hu, H. L. Liu and J. Xu, Direct electrochemistry of hemoglobinimmobilized on siliceous mesostructured cellular foam, *Sens. Actuators B.*, 2009,**138**, 545–549.

3 F. G. Parak and G. U. Nienhaus, Myoglobin, a paradigm in the study of proteindynamics, *Chem Phys. Chem*., 2002, **3**, 249–254.

4 A. K. M. Kafi, G. Wu, P. Benvenuto and A. Chen, Highly sensitive amperometric H_2O_2biosensor based on hemoglobin modified TiO_2 nanotubes, *J. Electroanal. Chem.*, 2011, **662**, 64–69.

5 W. Chen, S. Cai, Q.Q. Ren, W. Wen and Y.D. Zhao, Recent advances in electrochemical sensing for hydrogen peroxide: a review, *Analyst*, 2012, **137**, 49–58.

6 Z. B. Mai, X. J. Zhao, Z. Dai, X. Y. Zou, Direct electrochemistry of hemoglobin adsorbed on self-assembled monolayers with different head groups or chain length, *Talanta*, 2010, **81**, 167-175.

7 D. Shan, E. Han, H. Xue and S. Cosnier, Self-assembled films of hemoglobin/laponite/chitosan: Application for the direct electrochemistry and catalysis to hydrogen peroxide, *Biomacromol.*, 2007, **8**, 3041-3046.

8 A. Heller, Electrical wiring of redox enzymes, *Acc. Chem. Res.*, 1990, **23**, 128-134.

9 S. Dong, Y. Zhu and S. Song, Electrode process of hemoglobin at a platinum electrode covered by brilliant cresyl blue, *Bioelectrochem. Bioenerg.*, 1989, **21**, 233–243.

10 M. Qian, C. Yang, J. Zhang and W. Pu, Immobilization of hemoglobin on platinum nanoparticles-modified glassy carbon electrode for H_2O_2 Sensing, *Wuhan Univ. J. Nat. Sci.*, 2010, **15**, 160-164.

11 R. Liu, Y. Han, F. Nie, R. Li and J. Zheng , Direct electrochemistry of hemoglobin and its biosensing for hydrogen peroxide on TiO_2–polystyrene nanofilms, *J. Iran. Chem. Soc.* 2014, **11**, 1569-1577.

12 S. Dong, N. Li, P. Zhang, Y. Li, Z. Chen and T. Huang, Fabrication of hemoglobin/ionic liquid modified carbon pasteelectrode based on the electrodeposition of gold nanoparticles/CdS quantum dots and its electrochemical application, *Elctroanalysis*, 2012, **24**, 1554–1560.

13 Y. Xu, J. Liang, C. Hu, F. Wang, S. Hu and Z. He, A hydrogen peroxide biosensor based on the direct electrochemistry of hemoglobin modified with quantum dots, *J. Biol. Inorg. Chem.*, 2007, **12**, 421–427.

14 W. Sun, S. Gong, F. Shi, L. Cao, L. Ling, W. Zheng and W. Wang, Direct electrochemistry and electrocatalysis of hemoglobin in graphene oxide and ionic liquid compositefilm, *Mater. Sci. Eng. C*, 2014, **40**, 235–241.

15 A. Banaei, H. Ghourchian, P. Rahimi, A. A. Moosavi Movahedi and R. Amjadi, Different electrochemical behavior of adult and fetal hemoglobin at ionic liquid-carbon nanotube nanocomposite, *J. Iran. Chem. Soc.*, 2015, **12**, 687-694.

16 Q. Liu, T. Zhang, L. Yu, N. Jia and D.P. Yang, 3D NanoporousAg@BSAcomposite microspheres as hydrogen peroxide sensors, *Analyst*, 2013, **138**, 5559−5562.

17 C. Hu, D. P. Yang, F. Zhu, F. Jiang, S. Shen and J. Zhang, Enzyme-labeled Pt@BSAnanocomposite as a facile electrochemical biosensing interface for sensitive glucose determination, *ACS Appl. Mater. Interfaces*, 2014, **6**, 4170−4178.

18 C. Hu, D. P. Yang, K. Xu, H. Cao, B. Wu, D. Cui and N. Jia, Ag@BSAcore/shell microspheres as an electrochemical interfacefor sensitive detection of urinary retinal-binding protein, *Anal. Chem.*, 2012, **84**, 10324−10331.

19 C. Hu, D. P. Yang, Z. Wang, P. Huang, X. Wang, D. Chen, D. Cui, M. Yang and N. Jia, Bio-mimetically synthesized Ag@BSA microspheres as a novel electrochemical biosensing interface for sensitive detection of tumor cells, *Biosens. Bioelectron.*, 2013, **41**,656−662.

20 M. Shamsipur, F. Molaabasi, M. Shanehsaz and A. A. Moosavi-Movahedi, Novel blue-emitting gold nanoclusters confinedin human hemoglobin and their use as fluorescent probes for copper(II) and histidine, *Microchim. Acta*, 2015, **182**, 1131–1141.

21 F. Molaabasi, S. Hosseinkhani, A. A. Moosavi-Movahedi and M. Shamsipur, Hydrogen peroxide sensitive hemoglobin-capped gold nanoclusters as a fluorescence enhancing sensor for the label-free detection of glucose, *RSC Adv.*, 2015, **5**, 33123–33135.

22 R. C. William, and K. Y. Tsay, A convenient chromatographic method for the preparation of humanhemoglobin, *Anal. Biochem.*, 1973, **54**, 137–145.

23 E. Antonini and M. Brunori, The derivatives of ferroushemoglobin and myoglobin. In A. Neuberger, E.L. Tatum (Eds.), Hemoglobin and myoglobin in their reactions with ligands, vol 21, Amsterdam: North-Holland Publishing Co (pp. 13–39).

24 L. Jin, L. Shang, S. Guo, Y. Fang, D. Wen, L. Wang, J. Yin and S. Dong, Biomolecule-stabilized Au nanoclusters as a fluorescence probe for sensitive detection of glucose, *Biosens. Bioelectron.*, 2011, **26**, 1965-1969.

25 X. L. Guével, B. Hötzer, G. Jung, K. Hollemeyer, V. Trouillet and M. Schneide, Formation of fluorescent metal (Au, Ag) nanoclusters capped in bovine serum albumin followed by fluorescence and spectroscopy, *J. Phys. Chem. C*, 2011, **115**, 10955–10963.

26 F. C. Chilaka, C. O. Nwamba and A. A. Moosavi-Movahedi, Cation modulation of hemoglobin interaction with sodiumn-dodecyl sulfate (SDS). I: calcium modulation at pH 7.20, *Cell Biochem. Biophys.*, 2011, **60**, 187–197.

27 J. R. McDonald, Impedance Spectroscopy, Wiley, New York, 1987.

28 M. D. Levi and D. Aurbach, The behavior of polypyrrole-coated electrodes in propylene carbonate solutions, *J. Electrochem. Soc.*, 2002, **14**, 215–221.

29 R. K. Shervadani, A. Mehrjardi and N. Zamiri, A novel method for glucose determination based on electrochemical impedance spectroscopy using glucose-oxidase self-assembled biosensor, *Bioelctrochem.*, 2006, **69**, 201–208.

30 Q. Sheng, R. Liu and J. Zheng, Fullerene–nitrogen doped carbon nanotubes for the direct electrochemistry of hemoglobin and its application in biosensing, *Bioelectrochem.*, 2013, **94**, 39–46.

31 K. Liu, J. Zhang, G. Yang, C. Wang and J.-J. Zhu, Direct electrochemistry and electrocatalysis of hemoglobin based on poly(diallyldimethylammonium chloride) functionalized grapheme sheets/room temperature ionic liquid composite film, *Electrochem. Commun.*, 2010, **12**, 402–405.

32 J. Li, J. Tang, L. Zhou, X. Han and H. Liu, Direct electrochemistry and electrocatalysis of hemoglobin immobilized on polyacrylamide-P123 film modified glassy carbon electrode, *Bioelectrochem.*, 2012, **86**, 60–66.

33 Y. Wang, M. Tang, X. Lin, F. Gao and M. Li, Sensor for hydrogen peroxide using a hemoglobin-modified glassy carbon electrode prepared by enhanced loading of silver nanoparticle onto carbon nanospheres via spontaneous polymerization of dopamine, *Microchim. Acta*, 2012, **176**, 405–410.

34 Y. Zhang, H. Cao, W. Fei, D. Cui and N. Jia, Direct electrochemistry and electrocatalysis of hemoglobin immobilized into halloysite nanotubes/room temperature ionic liquid composite film, *Sen. Actuators B*, 2012, **162**, 143–148.

35 X. He, L. Zhou, E. P. Nesterenko, P. N. Nesterenko, B. Paull, J. O. Omamogho, J. D. Glennon and J. H. T. Luong, Porous graphitized carbon monolith as an electrode material for probing direct bioelectrochemistry and selective detection of hydrogen peroxide, *Anal. Chem.*, 2012, **84**, 2351−2357.

36 J.-Y. Sun, K.-J. Huang, S.-F. Zhao, Y. Fan and Z.-W. Wu, Direct electrochemistry and electrocatalysis of hemoglobin on chitosan-room temperature ionic liquid-TiO_2-graphene nanocomposite film modified electrode, *Bioelectrochem.*, 2011, **82**, 125–130.

37 W. Sun, S. Gong, F. Shi, L. Cao, L. Ling, W. Zheng and W. Wang, Direct electrochemistry and electrocatalysis of hemoglobin in graphene oxide and ionic liquid composite film, *Mater. Sci. Eng. C*, 2014, **40**, 235–241.

38 E. Laviron, Adsorption, autoinhibition and autocatalysis in polarography and in linear potential sweep voltammetry, *J. Electroanal. Chem.*, 1974, **52**, 355–393.

39 E. Laviron, General expression of the linear potential sweep voltammogram in the case of diffusionless electrochemical systems, *J. Electroanal. Chem.*, 1979, **101**, 19–28.

40 S. F. Wang, T. Chen, Z. L. Zhang, X. C. Shen, Z. X. Lu, D. W. Pang and K. Y. Wong, Direct electrochemistry and electrocatalysis of heme proteins entrapped in agarose hydrogel films in room-temperature ionic liquids, *Langmuir*, 2005, **21**, 9260–9266.

41 I. Yamazaki, T. Araiso, Y. Hayashi, H. Yamada, R. Makino, Analysis of acid–base properties of peroxidase and myoglobin, *Adv. Biophys.*, 1978, **11**, 249–281.

42 R. A. Kamin and G. S. Wilson, Rotating ring-disk enzyme electrode for biocatalysis kinetic studies and characterization of the immobilized enzyme layer, *Anal. Chem.*, 1980, **52**, 1198–1205.

43 Y. Zhang, H. Cao, W. Fei, D. Cui and N. Jia, Direct electrochemistry and electrocatalysis of hemoglobin immobilized into halloysite nanotubes/room temperature ionic liquid composite film, *Sens. Actuators B*, 2012, **162**, 143–148.

44 Q. L. Wang, G. X. Lu and B. J. Yang, Direct electrochemistry and electrocatalysis of hemoglobin immobilized on carbon paste electrode by silica sol–gel film, *Biosens. Bioelectron.*, 2004, **19**, 1269–1275.

45 J. Xu, W. Li, Q. Yin, H. Zhong, Y. Zhu and L. Jin, Direct electron transfer and bioelectrocatalysis of hemoglobin on nano-structural attapulgite clay-modified glassy carbon electrode, *J. Colloid Interface Sci.*, 2007, **315**, 170–176.

46 M. Shamsipur, M. Asgari, M. Ghannadi Maragheh and A. A. Moosavi-Movahedi, A novel impedimetric nanobiosensor for low level determination of hydrogen peroxide based on biocatalysis of catalase, *Bioelectrochem.*, 2012, **83**, 31–37.

47 M. Shamsipur, M. Asgari, M. F. Mousavi and R. Davarkhah, A novel hydrogen peroxide sensor based on the direct electron transfer of catalase immobilized on nano-sized NiO/MWCNTs composite film, *Electroanalysis*, 2012, **24**, 357–367.

48 E. Koposov, X. Liu, A. Kisner, Y. Ermolenko, G. Shumilova, A. Offenhäusser, Y. Mourzin, Bioelectrochemical systems with oleylamine-stabilized gold nanostructures and horseradish peroxidase for hydrogen peroxide sensor, *Biosens. Bioelectron.*, 2014, **57**, 54–58.

49 Y. Han, J. Zheng, S. Dong, A novel nonenzymatic hydrogen peroxide sensor based on Ag–MnO_2–MWCNTs nanocomposites, *Electrochim. Acta*, 2013, **90**, 35–43.

50 M. M. Khan, S. A. Ansari, J. Lee and M. H. Cho, Novel Ag@TiO_2nanocomposite synthesized by electrochemically active biofilm for nonenzymatic hydrogen peroxide sensor, *Mater. Sci. Eng. C*, 2013, **33**, 4692–4699.

51 S. K. Maji, S. Sreejith, A. K. Mandal, X. Ma and Y. Zhao, Immobilizing gold nanoparticles in mesoporous silica covered reduced graphene oxide: A hybrid material for cancer cell detection through hydrogen peroxide sensing, *ACS Appl. Mater. Interfaces*, 2014, **6**, 13648–13656.

52 X. Chen, B. Guo, P. Hu and Y. Wang, A non-enzymatic hydrogen peroxide sensor based on gold nanoparticles/carbon nanotube/self-doped polyaniline hollow spheres, *Electroanalysis*, 2014, **26**, 1513–1521.

53 N. Butwong, L. Zhou, W. Ng-Eontae, R. Burakham, E. Moore, S. Srijaranai, J. H. T. Luongd, and J. D. Glennon, A sensitive non-enzymatic hydrogen peroxide sensor using cadmium oxide nanoparticles/multiwall carbon nanotube modified glassy carbon electrode, *J. Electroanal. Chem.*, 2014, **717**, 41–46.

54 X. Li, X. Liu, W. Wang, L. Li and X. Lu, High loading Pt nanoparticles on functionalization of carbon nanotubes for fabricating non-enzyme hydrogen peroxide sensor, *Biosens. Bioelectron.*, **59**, 2014, 221–226.

55 F. Lorestani, Z. Shahnavaz, P. Mn, Y. Alias and N. S. A. Manan, One-step hydrothermal green synthesis of silver nanoparticle-carbon nanotube reduced-graphene oxide composite and its application as hydrogen peroxide sensor, *Sens. Actuators B*, 2015, **208**, 389–398.

56 A. N. Kawde, M. Aziz, N. Baig and Y. Temerk, A facile fabrication of platinum nanoparticle-modified graphite pencil electrode for highly sensitive detection of hydrogen peroxide, *J. Electroanal. Chem.*, 2015, **740**, 68–74.

57 Y. Li, Y. Zhong, Y. Zhang, W. Weng and S. Li, Carbon quantum dots/octahedral Cu_2O nanocomposites for non-enzymatic glucose and hydrogen peroxide amperometric sensor, *Sens. Actuators B*, 2015, **206**, 735–743.

58 K. C. Lin, T. H. Wu and S. M. Chen, Electrocodeposition of silver and silicomolybdate hybrid nanocomposite for non-enzymatic hydrogen peroxide sensor, *RSC Adv.*, 2015, **5**, 41224-41229.

59 S. Dong, J. Xi, Y. Wu, H. Liu, C. Fu, H. Liu and F. Xiao, High loading MnO_2 nanowires on graphene paper: Facile electrochemical synthesis and use as flexible electrode for tracking hydrogen peroxide secretion in live cells, *Anal. Chim. Acta*, 2015, **853**, 200–206.

60 Y. Wang, Z. Wang, Y. Rui, M. Li, Horseradish peroxidase immobilization on carbon nanodots/CoFe layered double hydroxides: Direct electrochemistry and hydrogen peroxide sensing, *Biosens. Bioelectron.*, 2015, **64**, 57–62.

61 X. Cui, S. Wu, Y. Li and G. Wan, Sensing hydrogen peroxide using a glassy carbon electrode modified with in-situ electrodeposited platinum-gold bimetallic nanoclusters on a graphene surface, *Microchim. Acta*, 2015, **182**, 265-272.

Figure Legends:

Fig. 1. TEM images of Hb-AuNCs.

Fig. 2. (A) FT–IR spectra of Hb and AuNC@Hb films and (B) UV-Vis absorption spectra of Hb and Hb@AuNCs in 0.05 M PBS buffer of pH,7.4.

Fig. 3. (A) Nyquist plots for GCE (a) and Hb-AuNCs/Chit/GCE (b). (B) Plot of impedance vs $\omega^{-1/2}$, in the presence of 5 mM $[Fe(CN)_6]^{3-/4-}$ and 0.1 M KCl at a frequency range of 10^5- 0.1 Hz.

Fig.4. Cyclic voltammograms of GC/Hb/Chit and GC/AuNC@Hb/Chit in absence (a, b) and presence (á, b́) of a 12.0 µM H_2O_2 in 0.1 M PBS of pH 7.4 at a scan rate of 50 mV s^{-1}.

Fig. 5. Possible mechanism of electrocatalytic reduction of hydrogen peroxide.

Fig .6. (A) Cyclic voltammgrams of the modified electrode in a 0.05 M PBS of pH 7.4 at various scan rates of 20, 50, 100, 150, 220, 300, 400 and 500 mV s^{-1}. (B) Variation of peak currents vs potential scan rate.

Fig. 7. CVs of proposed biosensor in 0.05 M PBS of different pHs at a scan rate 50 mV s^{-1}.

Fig. 8. (A) Amperometric response of biosensor at a rotating modified electrode in the presence of different H_2O_2 concentrations. (B) Plot of amperometric currents vs H_2O_2 concentrations.

Fig. 9. Potential cycling of biosensor between -0.8 and 0.1 V in 0.05 M PBS of pH 6.8 at a scan rate of 50 mV s^{-1}: (a) first cycle, (b) after 80 continuous cycles.

Table 1 Comparison of linear range and limit of detection of different electrochemical Sensors reported for hydrogen peroxide determination.

Electrode	Method	Linear range	LOD	Ref.
GCE/MWCNTs/[bmim][PF_6]/CAT	Impedimetry	5.0 nM–1.7 μM	0.25 nM	46
GCE/MWCNTs/NiO/CAT	Impedimetry	19–170 nM	2.4 nM	47
GC/MWCNT-NiO/CAT	Amperometry	0.20–2.53 mM	19 mM	47
Ag–MnO_2–MWCNTs	Voltammetry	5.0 μM-10.4 mM	1.7 μM	49
NanoAg@TiO_2/GCE	Voltammetry	0.83-43.3 μM	0.83 μM	50
AuNPs-MesSi/GrO	Voltammetry	0.5 μM-50 mM	60 nM	51
GNPs/CNTs/Self-Doped PA Hollow Spheres	Chronoamperometry	5 μM- 0.225 mM	0.4 μM	52
CdNPs/MWCNTs/GCE	Voltammetry	0.5- 200 μM	0.1 μM	53
PtNPs/CNTs	Voltammetry	5.8 nM-1.1 mM	1.9 nM	54
OA-AuNWs/HRP	Voltammetry	20-500 μM	5 μM	48
OA-AuNPs/HRP	Voltammetry	20-500 μM	8 μM	48
AgNPs/CNTs/GrO	Voltammetry	0.1–100 mM	0.9 μM	55
PtNPs/GPE	Amperometry	5 μM-5.3 mM	2.8 μM	56
CQDs-Cu_2O NC	Voltammetry	0.03-15.0 mM	22.8 μM	57
Ag-Si-Mo NC	Amperometry	50 μM-24 mM	0.1 mM	58
MnO_2 NWs-GrP	Amperometry	0.1–45.4 mM	10 μM	59
HRP/CDs/LDHs/GCE	Voltammetry	0.1–23.1 μM	0.04 μM	60
Pt-AuNCs/Gr	Voltammetry	15 nM-8.73 μM	8.0 nM	61
Hb-AuNCs/Chit/GCE	Amperometry	55-700 nM	16.5 nM	This work

GCE, Glassy carbon electrode; MWCNTs, Multiwall carbon nanotubes; Cat, Catalase; NPs, Nanoparticles; Gr, Graphene; Mes, Mesoporous; OA, Oleylamine; HRP, Horseradish peroxidase; GPE, Graphite pencil electrode; CQDs, Carbon quantum dots; NC, Nanocomposite; GrP, graphen paper; NCs, Nanoclusters; Chit, Chitosan.

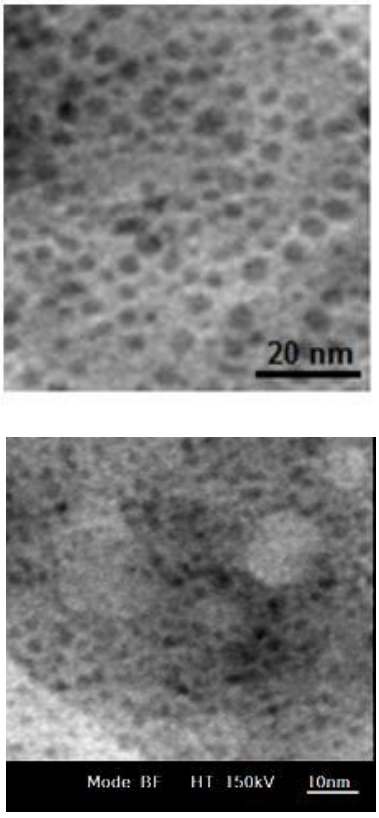

Fig. 1

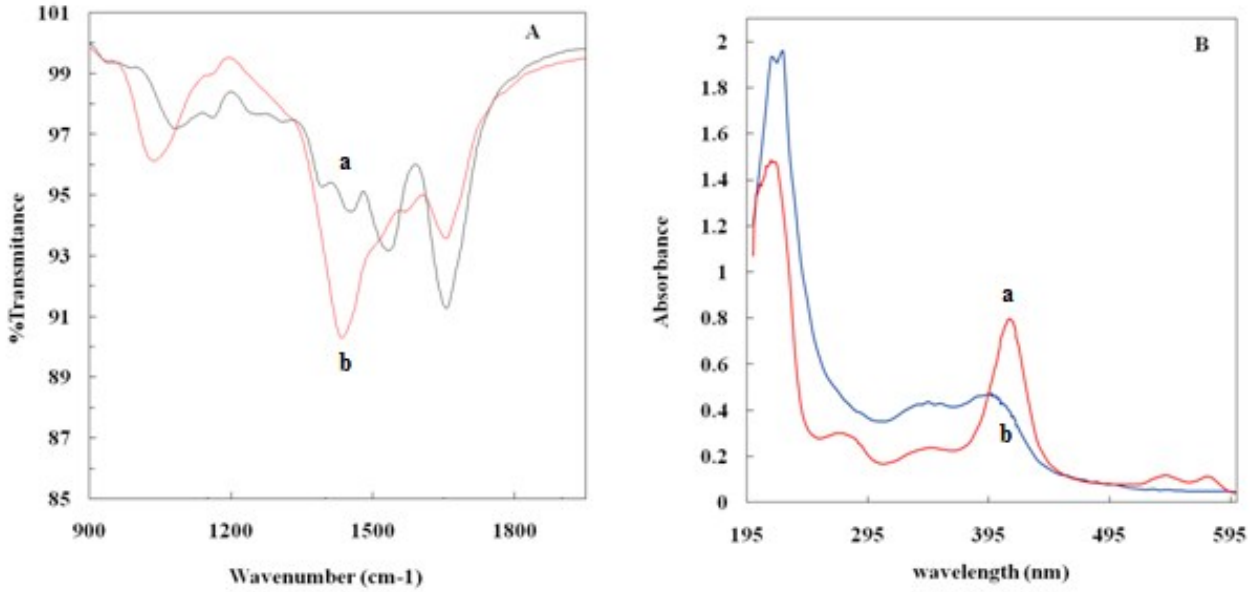

Fig. 2

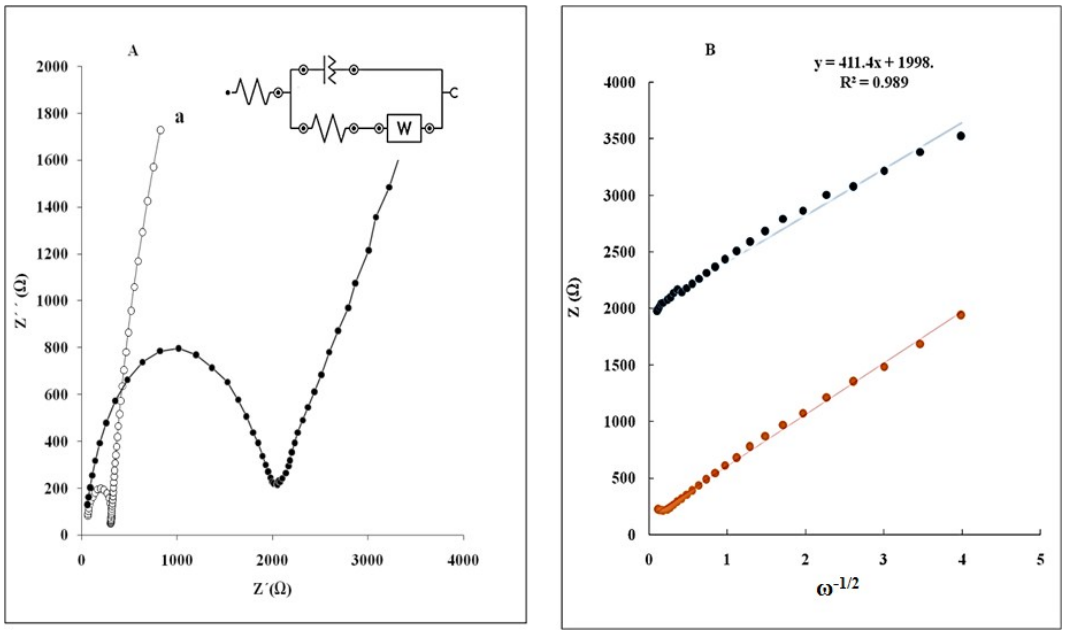

Fig. 3

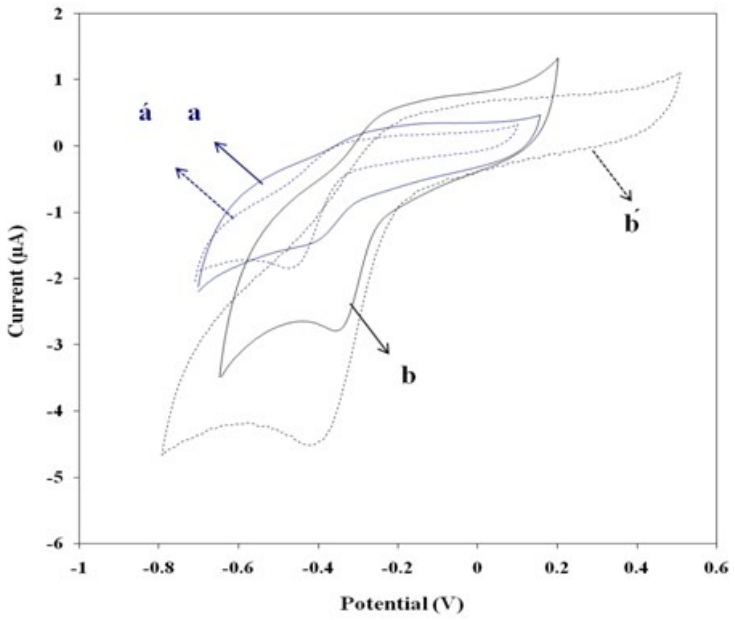

Fig. 4

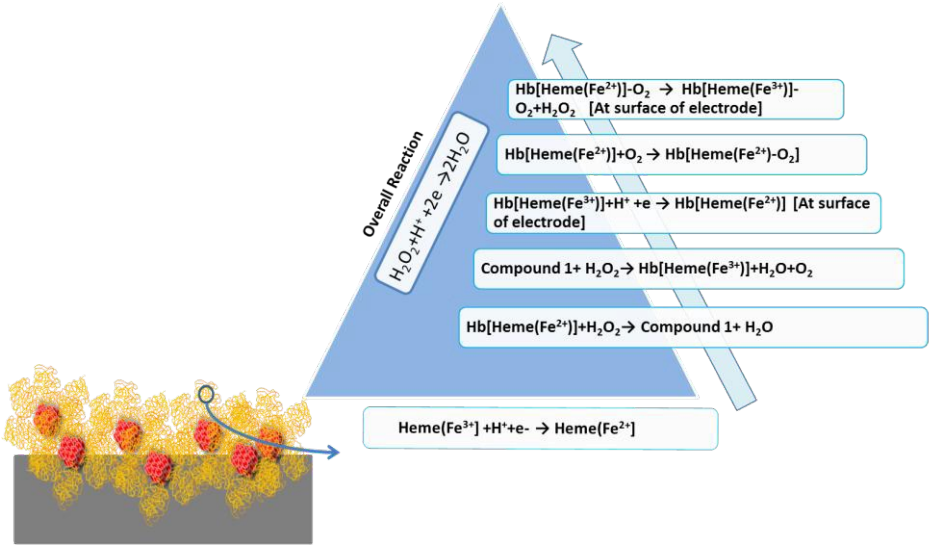

Fig. 5

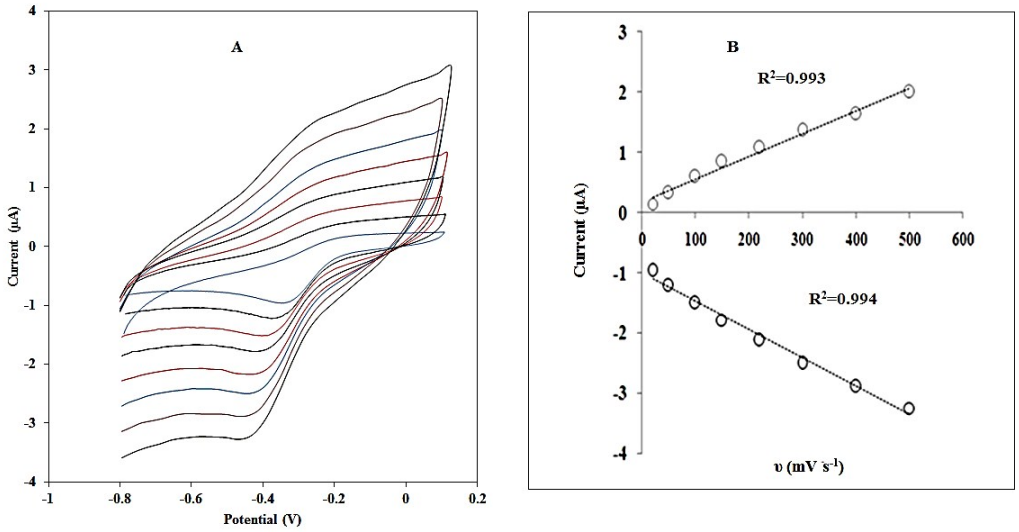

Fig. 6

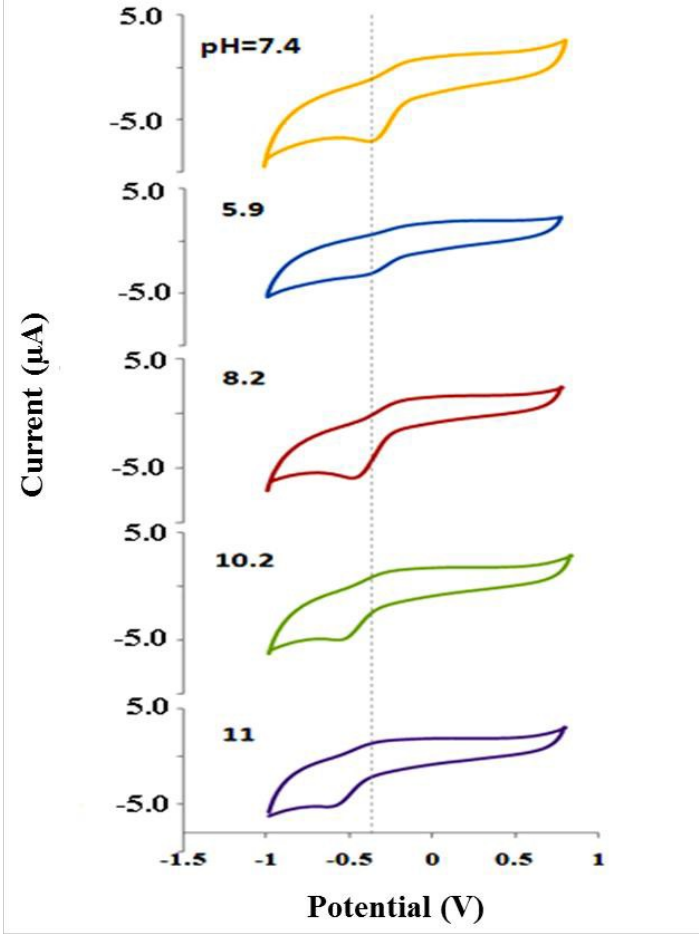

Fig. 7

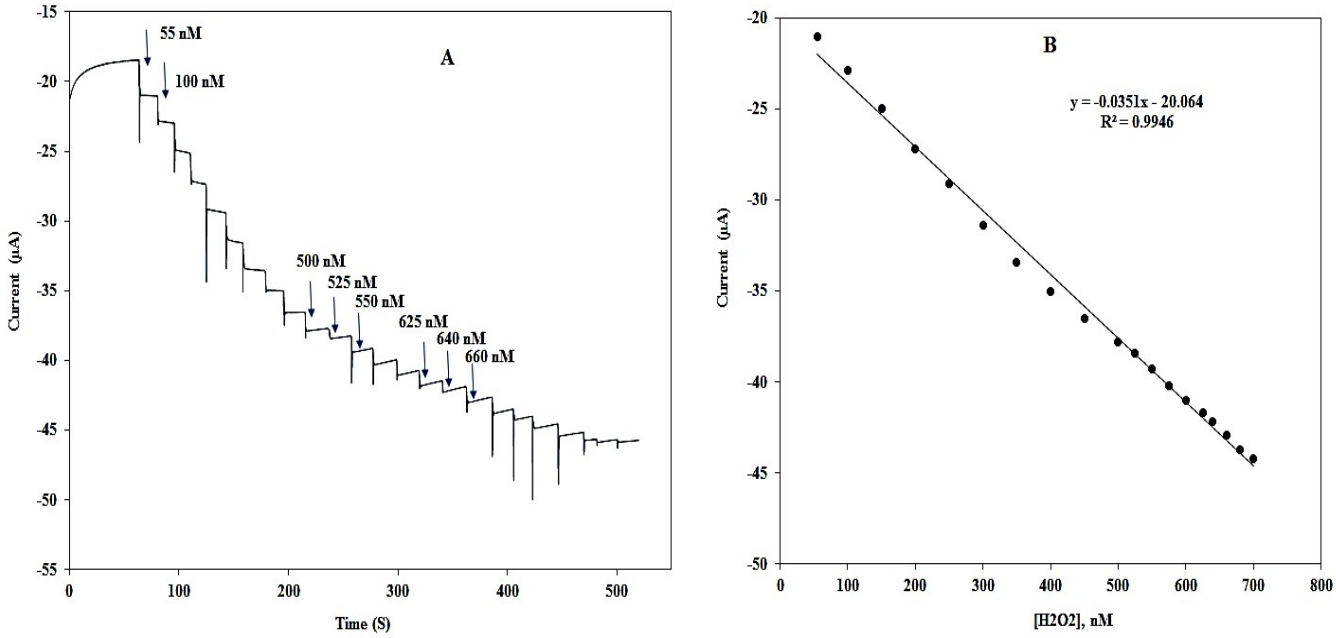

Fig. 8

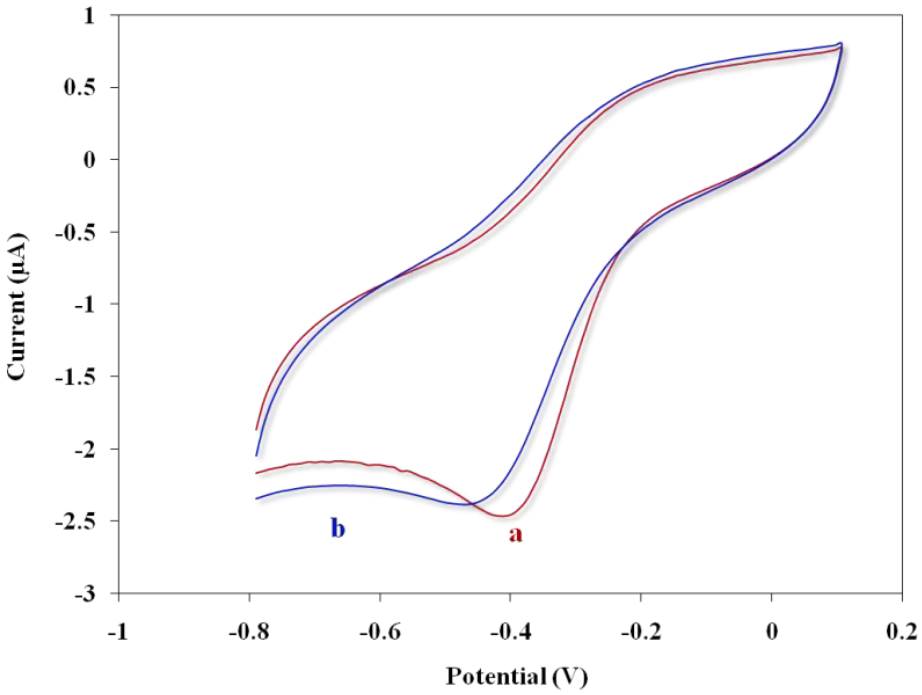

Fig. 9